A sulfur-rich pi-electron acceptor derived from 5,5 '-bithiazolidinylidene: charge-transfer complex vs. charge-transfer salt

Y Le Gal, M Rajkumar, A Vacher, V Dorcet, T Roisnel, M Fourmigue, F Barriere, T Guizouarn, D Lorcy

▶ **To cite this version:**

Y Le Gal, M Rajkumar, A Vacher, V Dorcet, T Roisnel, et al.. A sulfur-rich pi-electron acceptor derived from 5,5 '-bithiazolidinylidene: charge-transfer complex vs. charge-transfer salt. CrystEngComm, 2016, 18 (21), pp.3925–3933. 10.1039/c6ce00772d . hal-01338503

HAL Id: hal-01338503

https://univ-rennes.hal.science/hal-01338503

Submitted on 27 Oct 2016

HAL is a multi-disciplinary open access archive for the deposit and dissemination of scientific research documents, whether they are published or not. The documents may come from teaching and research institutions in France or abroad, or from public or private research centers.

L'archive ouverte pluridisciplinaire **HAL**, est destinée au dépôt et à la diffusion de documents scientifiques de niveau recherche, publiés ou non, émanant des établissements d'enseignement et de recherche français ou étrangers, des laboratoires publics ou privés.

A sulfur-rich π-electron acceptor derived from 5,5'-bithiazolidinylidene: charge-transfer complex *vs*. charge-transfer salt

Yann Le Gal, Mangaiyarkarasi Rajkumar, Antoine Vacher, Vincent Dorcet, Thierry Roisnel, Marc Fourmigué, Frédéric Barrière, Thierry Guizouarn and Dominique Lorcy*

Institut des Sciences Chimiques de Rennes, UMR 6226 CNRS-Université de Rennes 1, Matière Condensée et Systèmes Electroactifs (MaCSE), Campus de Beaulieu, Bât 10A, 35042 Rennes cedex, France. E-mail: Dominique.lorcy@univ-rennes1.fr.

Abstract

Novel π-electron acceptors are still highly desirable for the formation of conducting salts or as n-dopable semiconductors. We describe here two synthetic approaches to substitute a dicyanovinylidene group, $C=C(CN)_2$ for a thioketone (C=S) in the recently described DEBTTT acceptor where DEBTTT stands for (*E*)-3,3'-diethyl-5,5'-bithiazolidinylidene-2,4,2',4'-tetrathione. These electron withdrawing groups enhance the electron accepting ability as demonstrated through electrochemical investigations, without hindering the formation of short intra- and intermolecular S•••S contacts in the solid state. Association of this acceptor **1** with tetramethyltetrathiafulvalene (TMTTF) and decamethylferrocene ($Fe(Cp^*)_2$) afforded 1:1 adducts which were analyzed by single crystal X-ray diffraction. Combined with vibrational and magnetic properties, it appears that [TMTTF][**1**] behaves as a neutral charge-transfer complex while [$Fe(Cp^*)_2$][**1**] is an ionic salt. The concentration of the spin density on the exocyclic sulfur atoms in $\mathbf{1}^{-\bullet}$, favors the setting of direct antiferromagnetic interactions in [$Fe(Cp^*)_2$][**1**].

Introduction

Organic electron acceptors with a π-conjugated framework have focused a lot of attention either for the elaboration of conducting materials,[1] or for the development of next generation of organic field-effect transistors (OFETs).[2,3,4,5] The elaboration of conducting materials can result from the redox reaction between a π-electron donor and a π-electron acceptor as in the prototypical TTF•TCNQ charge transfer (CT) salt.[1] These molecular materials are formed if the oxidizing agent, the acceptor, and the reducing agent, the donor, exhibit the appropriate electron affinity (EA) and ionization potential (IP) respectively to allow a partial or total CT between the donor and the acceptor.[6,7] The IP of the donor and the EA of the acceptor can be estimated electrochemically from their redox potential values in solution and the difference between the oxidation potential of the donor (E_{ox}) and the reduction potential of the acceptor (E_{red}) indicates if a CT is susceptible to occur.[6,7] Within this framework, we recently reported the synthesis of a sulfur-rich electron acceptor, the DEBTTT [(*E*)-3,3′-diethyl-5,5′-bithiazolidinylidene-2,4,2′,4′-tetrathione], which has proved to be a valuable acceptor in the preparation of CT salt with $[Fe(Cp^*)_2]$.[8]

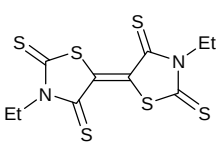

DEBTTT

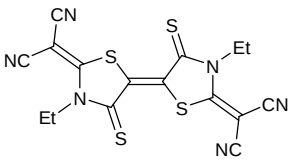

1

It is worth mentioning that DEBTTT is also a valuable candidate in the elaboration of air-stable n-channel organic field-effect transistors, since the rare presence of sulfur atoms in such acceptors favor stronger intermolecular interactions for enhanced charge mobilities.[9] Nevertheless, the oxidizing ability of this acceptor is below those traditionally used to oxidize tetrathiafulvalene derivatives. Thus, there is an interest in extending this new family of

acceptors, by increasing their electron acceptor ability. In this context, we have developed different approaches for the synthesis of DEBTTT and extended it to novel derivatives, either by replacing sp^2 sulfur atoms by more electronegative oxygen atoms or by modifying the nitrogen alkyl substituents.[10] However, these modifications didn't significantly enhance their electron acceptor ability. Herein, we wish to present another structural modification on the DEBTTT prototype, in order to increase the overall accepting ability. For instance, we substituted the thioketone (C=S) at the 2 position of the thiazole rings by a dicyanovinylidene group, $C=C(CN)_2$. The presence of this well-known electron withdrawing group should increase the overall electron acceptor character of the molecule. Accordingly, we report the syntheses and characterizations of a novel electron acceptor the (*E*)-3,3′-diethyl-5,5′-bithiazolidinylidene-4,4′-dithione-2,2'-di(dicyanovinylidene) **1**. Moreover, we also investigated the ability of this acceptor to form CT complexes with different donor molecules, namely tetramethyltetrathiafulvalene (TMTTF) and decamethylferrocene $[Fe(Cp^*)_2]$.

Results and Discussion

The target acceptor skeleton is prepared starting from the thiazole ring bearing a protected dithiolene ligand **2** as reported in Scheme 1.[11] In order to graft a dicyanovinylidene group on the thiazole core, we first transformed the thioketone **2** into a thiazolium salt **3** by adding to a solution of **2** in $CHCl_3$, trimethylorthoformate and borontrifluoride diethyletherate (Scheme 1).[12] The thiazolium salt **3** in the presence of NEt_3 reacts with malononitrile in refluxing dichloromethane to give the dicyanovinylidene **4** in 60% yield.[13]

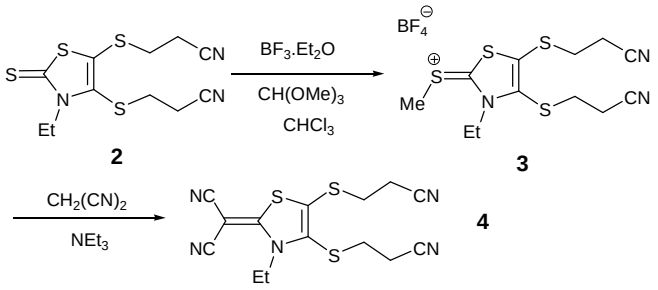

Scheme 1. Synthetic path to the malononitrile derivative **4**.

Crystals of sufficient quality for an X-ray diffraction study were obtained by slow concentration of a CH_2Cl_2 solution of **4**. The molecular structure is reported in Figure 1. The crystal structure of **4** reveals that the thiazole core is planar, while the cyanoethyl and ethyl substituents point out of the plane. The dicyanovinylidene group is also slightly distorted presumably due to some steric hindrance between the ethyl substituent and one cyano group.

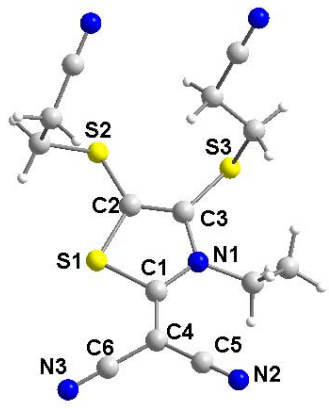

Figure 1. Molecular structure and numbering schemes for **4**.

As previously reported,[10] an efficient synthesis of the acceptor skeleton consists in transforming the protected dithiolene ligand with cyanoethyl groups into the protected dithiolene ligand within a dithiole-2-one cycle. Then, by simply heating the bicyclic structure into refluxing toluene, the acceptor skeleton is formed. Hence, we attempted to form first the bicyclic structure starting from **4** (Scheme 2). Thus, we deprotected the dithiolene ligand by

treating **4** with LDA and then we added triphosgene in the medium. During the work up we noticed the evolution of the bicyclic structure **5** into a highly colored derivative. Assuming that the bicyclic structure **5** was transformed easily to the acceptor **1**, due to the presence of the dicyanovinylidene group, we heated the reaction mixture into toluene without isolating **5**. Purification was achieved through column chromatography affording dark purple crystals after slow evaporation of the solution. The acceptor **1** was therefore obtained directly from **4** in 48% yield.

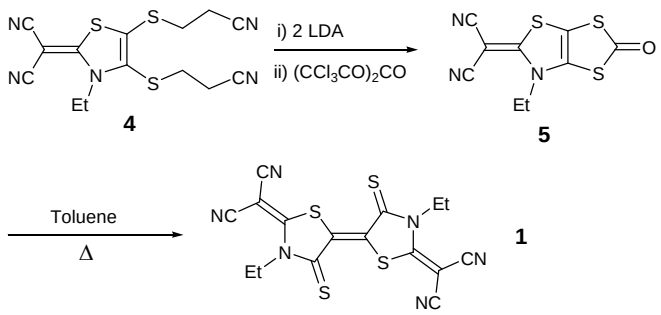

Scheme 2. Synthetic path to the electron acceptor **1**.

We also attempted another approach for the synthesis of **1** starting from preformed DEBTTT. Indeed, it has been reported earlier that thiocarbonyl derivatives can react with tetracyanoethylene oxide to afford dicyanovinyl derivatives[14] and this reactivity has been used by Gompper *et al.* to convert dithiole-2-thione derivatives into the corresponding dicyanomethylene derivatives.[15] Applied to DEBTTT, this strategy also raises the question of selectivity as two different thiocarbonyl groups are present. The reaction of DEBTTT with tetracyanoethylene oxide (Scheme 3) was carried out in toluene at 0-20°C in the presence of an excess of tetracyanoethylene oxide. Using these conditions we successfully isolated **1** in 56% yield.

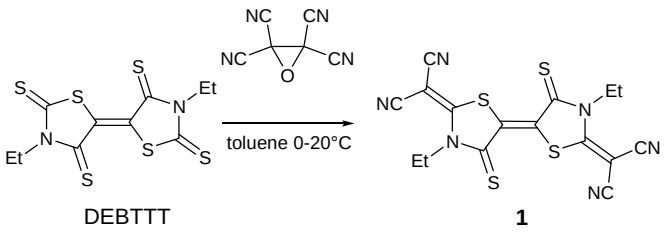

Scheme 3. Alternative synthesis of **1** from the preformed electron acceptor DEBTTT.

The molecular structure of neutral **1** obtained from single crystal X-ray diffraction is given in Figure 2. This compound exhibits a planar skeleton with a *trans* arrangement of the thiazole rings. Short (1,5) intramolecular S1•••S2 contacts at 2.877(3) Å can be noticed and the ethyl groups are pointing out of the plane. The C1=C1 central bond length amounts to 1.352(4) Å. Herein, the dicyanovinylidene groups are coplanar with the acceptor skeleton and the C6–C7 bond length is slightly shorter than in precursor **4** as it amounts to 1.378(4) Å instead of 1.414(3) Å, a possible indication of an enhanced delocalization.

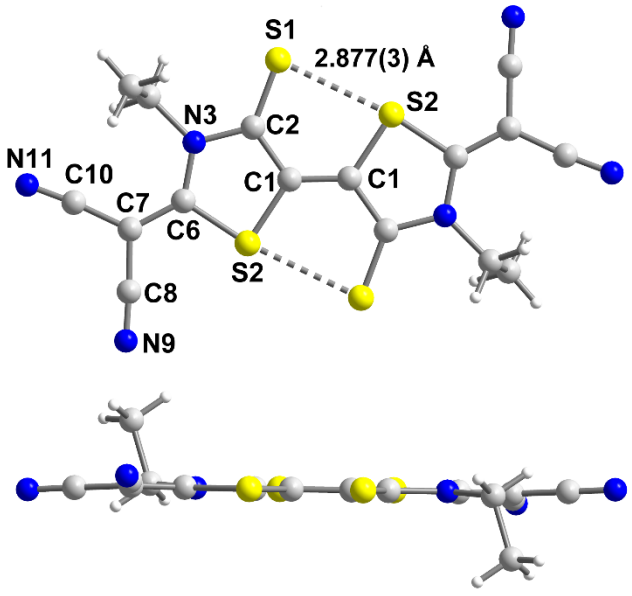

Figure 2. Molecular structure and numbering schemes for **1** (top), and side view (bottom).

With this new electron acceptor in hand, and before CT salt experiments, we first evaluated its electronic properties, as detailed below. The redox properties of **1** were analyzed

by cyclic voltammetry in CH_2Cl_2 using nBu$_4$NPF$_6$ as supporting electrolyte. The cyclic voltammogram (CV) of this acceptor (Figure 3) exhibits two reversible monoelectronic reduction waves assigned to the reversible reduction of the neutral species to the anion radical and then to the dianion at $E_1 = 0.06$ V and $E_2 = –0.34$ V *vs*. SCE respectively. It is of interest to compare these redox potentials with those of the well-known π-electron acceptor such as TCNQ (tetracyanoquinodimethane) (E_1 = 0.18 and E_2 = –0.37 V *vs.* SCE), as well as the sulfur analogue DEBTTT (E_1 = –0.05 V and E_2 = –0.44 V *vs* SCE in CH_2Cl_2).[8] These redox potentials show that **1** exhibits a slightly lower acceptor character than TCNQ, but that it is a stronger acceptor than DEBTTT as the first reduction potential is anodically shifted by 110 mV. Thus, we succeeded in improving the accepting ability through the introduction of two dicyanovinylidene groups.

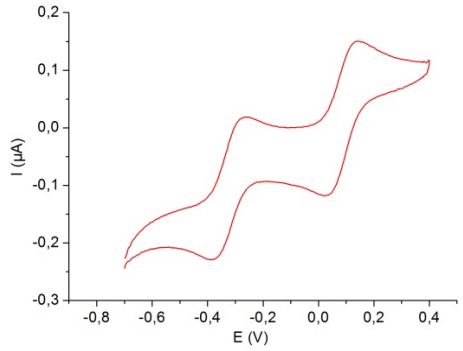

Figure 3. Cyclic voltammogram of **1** (CH_2Cl_2, nBu$_4$NPF$_6$, V vs SCE, Pt, 100 mV s^{-1})

UV-vis-NIR spectroelectrochemical investigations were carried out on a dichloromethane solution of **1** (c = 6 × 10^{-4} M) with nBu$_4$NPF$_6$ as supporting electrolyte (Figure 4). The neutral compound exhibits absorption bands in the UV-vis range from 250 nm to 600 nm. Gradual reduction from neutral to radical anion species, **1**$^{-\bullet}$, leads to a decrease of UV visible absorption bands at λ = 457 and 543 nm, concomitantly to the

increase of the bands at λ = 404 and 582 nm and the growth of two new bands at λ = 665 and 800 nm, characteristic of the formation of the anion radical species. Further reduction to the dianion species, $\mathbf{1}^{2-}$, leads to the decrease of all the absorption bands centered at 404, 582, 665 and 800 nm and the increase of a strong band at λ = 466 nm. These results are consistent with our previous work on the DEBTTT where a similar behavior was observed upon reduction.[10]

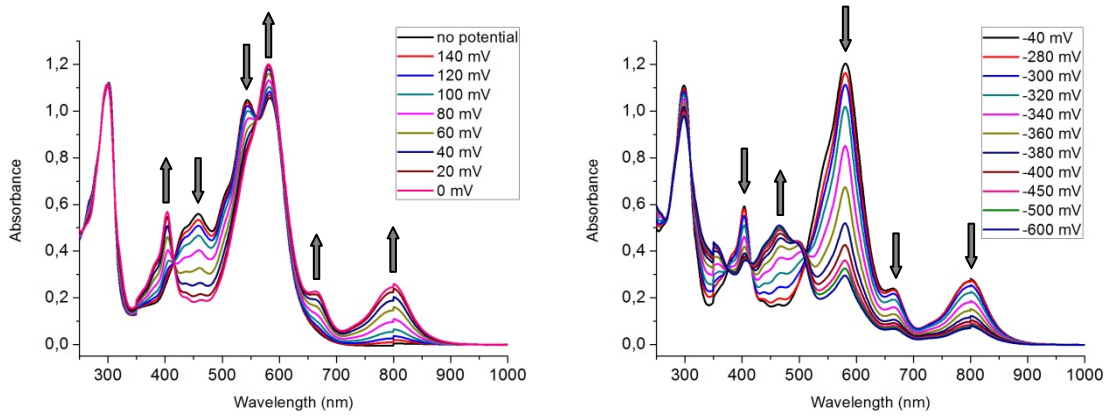

Figure 4. UV-vis-NIR absorption spectra monitored from 0.14 to 0V (left) and from –0.04 to –0.6 V (right) of the electrochemical reduction of **1** in dichloromethane with 0.2 M nBu$_4$NPF$_6$.

These investigations tend to indicate that the reduction processes for **1**, like for DEBTTT,[8] involve the central part of the molecules where upon reduction, modifications of the intramolecular bond lengths were shown to occur essentially on the central S=C–C=C–C=S fragment, as described in Scheme 4.

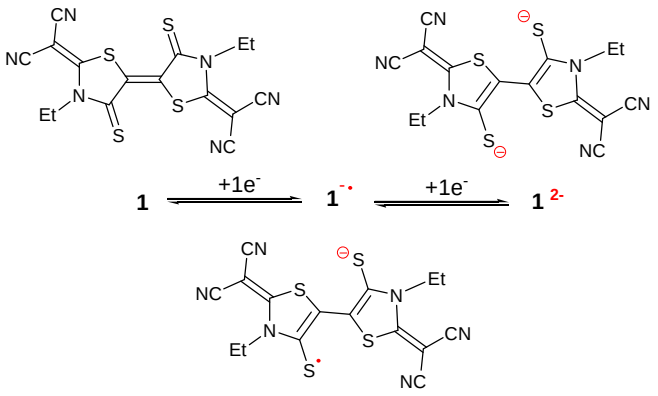

Scheme 4. The three redox states of **1**, neutral, radical anion and dianion

As two dicyanovinylidene groups are now present on the acceptor skeleton of **1**, we wondered if the IR nitrile stretching absorption bands in **1** will be sensitive to its reduction state. Indeed, a linear correlation has been established between the $\nu_{(C\equiv N)}$ frequencies and the reduction state for numerous TCNQ complexes and salts.[16] Accordingly, we performed a FTIR spectroelectochemical investigation on **1**, as well as on TCNQ itself for comparison purposes. This study was performed in dichloromethane with nBu$_4$NPF$_6$ as supporting electrolyte. The spectra obtained for **1** and TCNQ under the three redox states are reported in Figure 5.

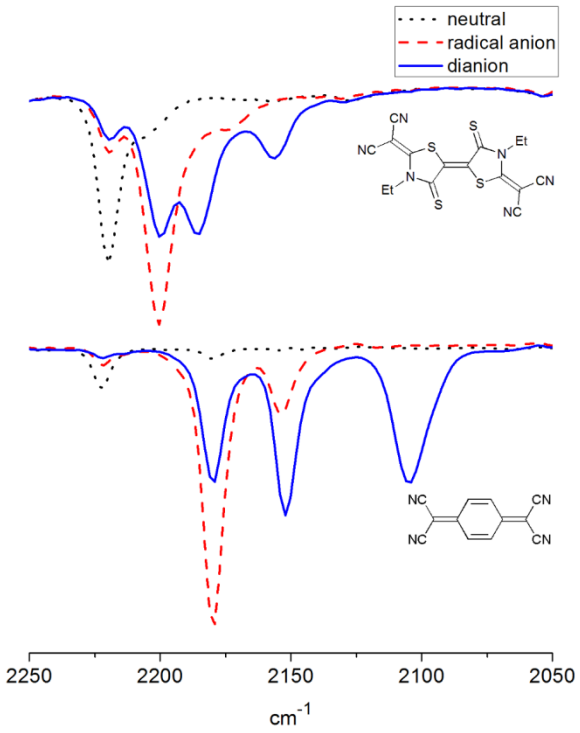

Figure 5. FTIR spectroelectrochemical spectra of **1** (top) and TCNQ (bottom) in dichloromethane with 0.1M nBu$_4$NPF$_6$.

In the neutral state, **1** exhibits a nitrile stretching vibration at $\nu_{C\equiv N}$ = 2219 cm^{-1}. Upon gradual reduction to the radical anion, **1**$^{-\bullet}$, a new band appears at lower energy at $\nu_{C\equiv N}$ = 2200 cm^{-1} concomitantly with the decrease of the band centered at 2219 cm^{-1}. Then, upon further reduction to the dianionic species, two new bands grow on the spectrum at even lower energy, 2186 and 2157 cm^{-1}, with a concomitant intensity decrease of the band localized at 2200 cm^{-1}. Concerning the TCNQ analyzed in the same experimental conditions, the neutral species exhibits the nitrile stretching vibration band at $\boldsymbol{\nu}_{C\equiv N}$ = 2222 cm^{-1}. This band is observed at a similar wavenumber than that observed for **1**, indicating a similar degree of conjugation in both acceptors. Upon reduction to the monoreduced species, TCNQ$^{-\bullet}$, two new bands centered at 2180 and 2154 cm^{-1} increase. Reduction to the dianionic species TCNQ^{2-} induces an intensity increase of the band at 2154 cm^{-1} together with the observation of a new band at 2105 cm^{-1}. Altogether a low energy shift of 117 cm^{-1} is observed from TCNQ to the

dianionic $TCNQ^{2-}$ while a much smaller shift of 62 cm^{-1} is observed between **1** and $\mathbf{1}^{2-}$, a further indication of a decreased participation of the malononitrile moieties in the reduction of **1**, when compared with TCNQ.

In order to get better insight into the reduction processes, DFT calculations [Gaussian09, B3LYP/6-311G**] were carried out on the neutral and the monoanionic species, that is **1** and $\mathbf{1}^{-\bullet}$, together with TCNQ for comparison purposes. Full geometry optimizations led to the molecular structure depicted in Figure 6 and the calculated bond lengths for the neutral and reduced species of **1** are collected in Table 1. The optimized geometry of **1** is in very good agreement with the experimental one obtained from X-ray diffraction regarding bond angles and bond distances (Table 1). The LUMO of **1** (Figure 6) is delocalized over the whole molecule as observed for the LUMO of TCNQ. Its energy lies in-between those of TCNQ and DEBTTT, confirming the electrochemical investigations (see above). We note however that the contribution of the malononitrile moieties to the LUMO do not exceed that of the corresponding sulfur atoms in DEBTTT. In other words, these malononitrile moieties in **1** exert a stronger inductive effect that the sulfur atoms of the thione in DEBTTT, but do not allow for a particularly extended charge delocalization in the reduced species. This is further confirmed by the evolution of the calculated bond lengths, between **1** and the anion radical $\mathbf{1}^{-\bullet}$. It essentially affects the central S=C–C=C–C=S fragment (Scheme 4), with the lengthening of the C=S and the C=C double bonds and concomitant shortening of the C–C bonds upon reduction, with also some minor variations on the other bonds of the acceptor skeleton.

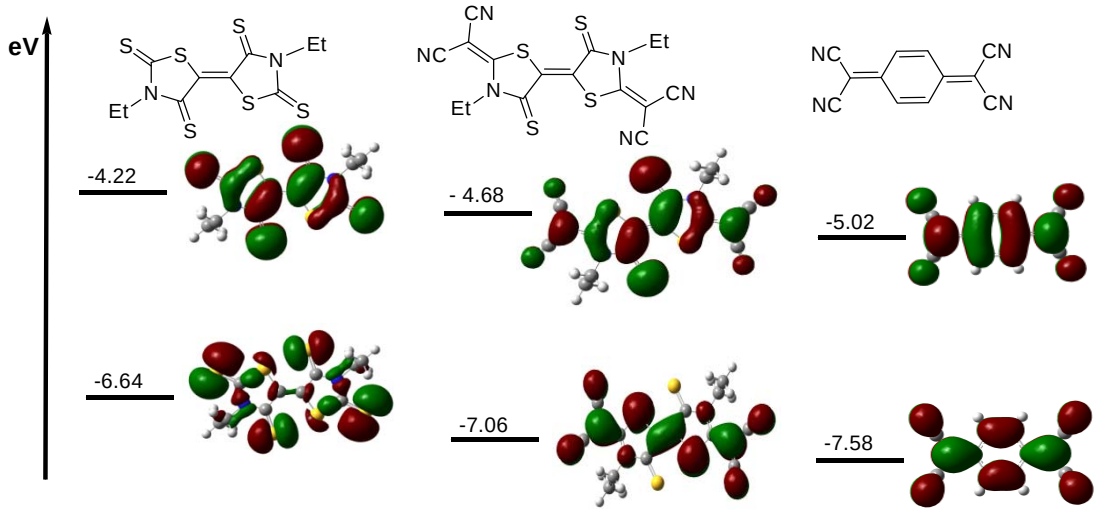

Figure 6. HOMO and LUMO of DEBTTT (left), **1** (middle) and TCNQ (right) shown with the same cut-off at 0.02 [e bohr^{-3}]$^{1/2}$.

Table 1. Selected experimental and calculated bond length (Å) for **1** and **1**$^{\bullet-}$.

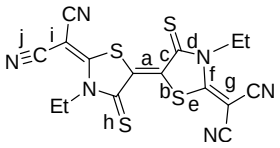

Bond	**1**	**1** calc.	**1** in [TMTTF][**1**] at RT	**1** in [TMTTF][**1**] at 150K	**1** in [(Cp*)$_2$Fc][**1**] at 150 K	**1**$^{\bullet-}$ calc.
a	1.373(3)	1.377	1.376(4)	1.384(6)	1.417(9)	1.408
b	1.7438(13)	1.763	1.741(2)	1.753(3)	1.754(5)	1.777
c	1.4555(18)	1.460	1.454(3)	1.448(5)	1.419(6)	1.415
d	1.3859(16)	1.391	1.393(3)	1.395(4)	1.391(6)	1.417
e	1.7583(14)	1.776	1.757(2)	1.760(3)	1.755(5)	1.761
f	1.3623(17)	1.368	1.355(3)	1.358(4)	1.341(7)	1.355
g	1.3820(19)	1.383	1.385(3)	1.392(4)	1.395(8)	1.405
h	1.6407(13)	1.658	1.639(2)	1.650(3)	1.680(4)	1.690
i	1.424(2)	1.421	1.426(3)	1.430(5)	1.426(8)	1.415
	1.428(2)	1.426	1.430(4)	1.431(5)	1.427(8)	1.420
j	1.134(2)	1.157	1.137(3)	1.151(5)	1.136(8)	1.159
	1.139(2)		1.147(3)	1.161(6)	1.147(9)	1.160

Charge transfer salts and complexes with electron donors

In order to form CT salts with this novel acceptor, we choose two electron donor molecules exhibiting different redox properties such as the tetramethyl tetrathiafulvalene (TMTTF), and the decamethylferrocene $Fe(Cp^*)_2$. Indeed, both donors can be reversibly oxidized to the monocharged species at E_{ox} = +0.26 V for TMTTF and at E_{ox} = –0.05 V for $Fe(Cp^*)_2$ and, demonstrating that these values, $Fe(Cp^*)_2$ is a stronger reducing agent than TMTTF. In solution, electron transfer is directly associated to the positive or negative value of the potential difference $\Delta E = E_{red}(\text{Acceptor}) - E_{ox}(\text{Donor})$. In the solid state, the extra stabilization brought to ionic structures can allow for a partial CT for negative ΔE values, in the approximate range $-0.30/-0.20 < \Delta E < 0$.[6b,17] With the first reduction potential of **1** measured at +0.06 V, we obtain with $Fe(Cp^*)_2$ a positive ΔE value of +0.11 V, anticipating a CT to an ionic salt. On the other hand, with the less reducing TMTTF molecule, ΔE amounts to –0.20 V, indicating a borderline situation.

The CT complexes were prepared by mixing an acetonitrile solution of **1** with a dichloromethane solution of the donor. After a couple of days and slow concentration of the solutions, deep dark crystals were obtained. X-ray crystal structure determinations carried out on single crystals reveal a stoichiometry of one donor with one acceptor in both compounds, formulated as [TMTTF][**1**] and $[Fe(Cp^*)_2][\mathbf{1}]$. Selected bond lengths of the acceptor skeleton in both CT salts are collected in Table 1. As shown in Figure 7, [TMTTF][**1**] (triclinic system, space group P–1) is organized into alternated stacks running along *a*. Short intermolecular S•••S contacts between the donor and acceptor molecules are identified as well as short S•••S contacts between the acceptor molecules along the *b* axis.

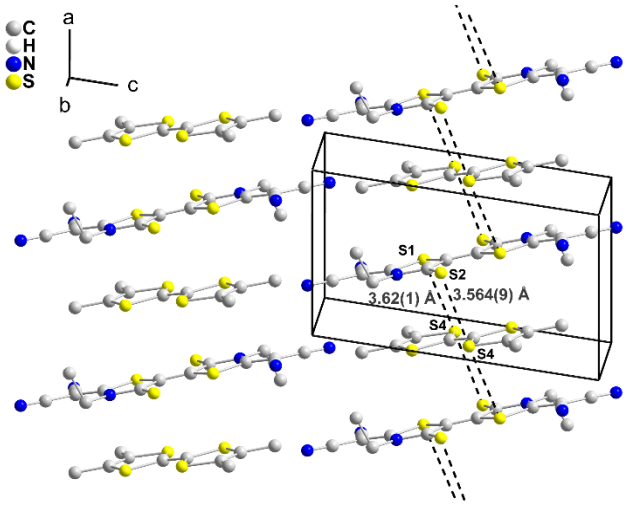

Figure 7. Solid state organization in [TMTTF][**1**]. The black dotted lines represent short (< 3.7 Å) intermolecular S•••S contacts. Hydrogen atoms were omitted for clarity.

The degree of CT between the donor and the acceptor **1** can be assessed from the analysis of the intramolecular bond lengths of the acceptor core within [TMTTF][**1**]. In the presence of TMTTF, the acceptor exhibits bond lengths similar to those found in neutral **1**, indicating the formation of a neutral charge-transfer complex, both in the room temperature and in the 150K X-ray structures. This is further confirmed by the structural characteristics of the TMTTF moiety itself. Indeed, the central C=C bond length of the TMTTF is also known to vary with the redox sate of the TTF core. Here in [TMTTF][**1**], this C=C bond length amounts to 1.353(5) Å, characteristic of a neutral TTF derivative.[18,19] This demonstrates that the redox difference mentioned above (ΔE = –0.20 V) is here too negative to stabilize a CT in this neutral compound that we will therefore describe as a CT *complex*.

In [Fe(Cp*)$_2$][**1**], alternated chains of donor and acceptor running along *c* are observed (Figure 8a). The intramolecular bond lengths (Table 1) in the acceptor **1** in [Fe(Cp*)$_2$][**1**] are strongly modified from the structure of the neutral compound, with the central C=C bond as well as the C=S bonds significantly lengthened, while the C–C bonds of

the thiazoline rings are significantly shortened. This confirms the presence of the reduced species $\mathbf{1}^{-\bullet}$ in $[Fe(Cp^*)_2][\mathbf{1}]$, in accordance with the electrochemical ΔE positive value at + 0.11 V (See above). A projection view of the unit cell along the stacking axis *c* (Figure 8a) demonstrates that these alternated columns interact laterally with each other, either along *a* or along (*a*+*b*). The lateral interactions along *a* can be described as *in-registry* (Figure 8b), with the shortest Fe…Fe distances found between an iron atom at (x,y,z) and a neighboring one at 8.659(1) Å (x+1, y, z) and 11.421(16) Å (x+1, y, z+1). On the other hand, the interactions between columns along the (*a*+*b*) direction adopt an *out-of-registry* pattern (Figure 8c), with larger Fe…Fe distances at 11.731(4) Å (with Fe at 0.5–x, 0.5+y, 1.5–z) and 13.020(3) Å (0.5–x, 0.5+y, 0.5–z). Comparison with the all-sulfur DEBTTT analog described earlier shows that, despite the large size of **1** relative to DEBTTT, the shortest Fe…Fe distance is observed here at 8.659 Å while it amounts to the larger 9.338 Å value in $[Fe(Cp^*)_2]$[DEBTTT].

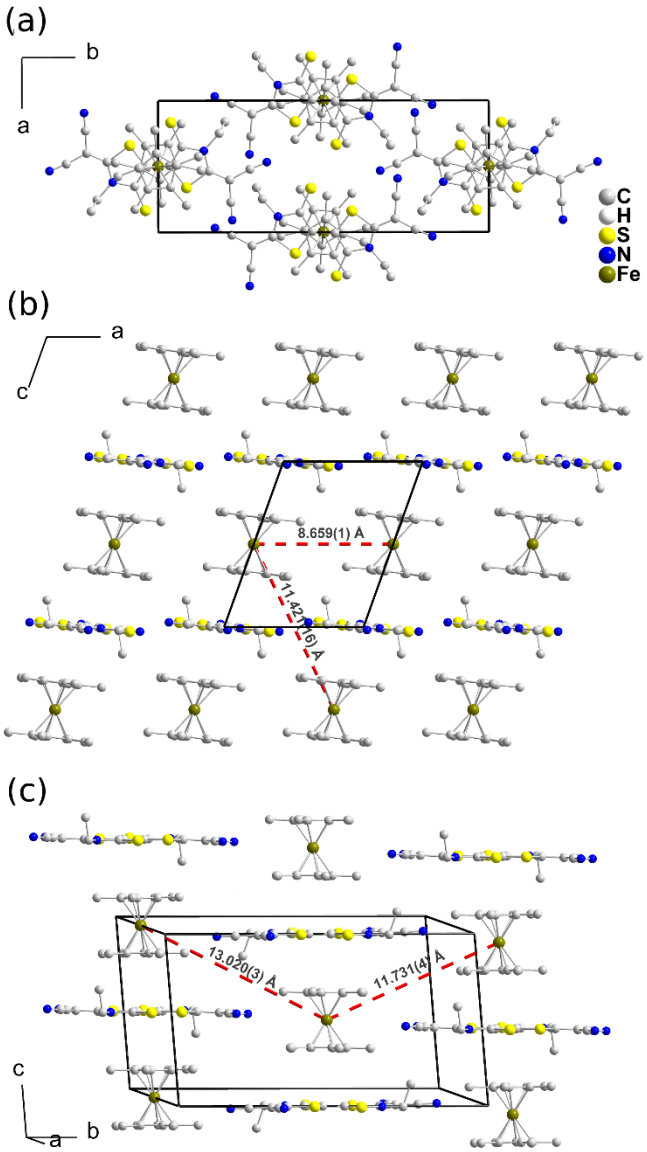

Figure 8. Different views of [Fe(Cp*)$_2$][**1**] with: (a) projection view along the stacking axis *c*, (b) detail of the in-registry alternated columns and (c) detail of the out-of-registry alternated columns. Hydrogen atoms were omitted for clarity.

Another possibility to determine the degree of CT between a donor and an acceptor exhibiting nitrile substituents is to investigate the nitrile stretching absorption band frequency (ν_{CN}). This approach has been widely used in the literature on crystalline TCNQ

salts as the strongest nitrile vibration band observed for a neutral TCNQ is found at ν_{CN} = 2227 cm^{-1} while it appears at lower energy value for $TCNQ^{-1}$ (ν_{CN} = 2185 cm^{-1}) in its $Na^{+}TCNQ^{-}$ salt.[16] We have shown above through spectroelectrochemical analyses that a sizeable shift of the ν_{CN} stretching frequency is observed upon reduction of **1** in solution. The IR spectra of solid acceptor **1** and both complexes, [TMTTF][**1**] and [$Fe(Cp^*)_2$][**1**], show ν_{CN} stretching frequencies at respectively 2215 cm^{-1}, 2213 cm^{-1} and 2198 cm^{-1}, confirming that the acceptor is neutral in the presence of the TMTTF while it is reduced with $Fe(Cp^*)_2$.

The magnetic susceptibility of [TMTTF][**1**] and [$Fe(Cp^*)_2$][**1**] were measured between 1.8 and 300 K on a SQUID magnetometer. No paramagnetism was found in the whole temperature range for [TMTTF][**1**], confirming that the complex is indeed neutral. Contrariwise, as shown in Figure 9, the χT product for [$Fe(Cp^*)_2$][**1**] amounts to 1.14 cm^3 K mol^{-1} at room temperature, in accordance with the expected value for the sum of two S = ½ species with g values close to 2 for the radical anion $\mathbf{1}^{-\bullet}$ and close to 2.7–2.8 for the decamethyl ferricinium cation.[20] The decrease of the χT product at lower temperatures indicates the presence of antiferromagnetic interactions. The χT data have been fitted to a Curie-Weiss law to give a Weiss constant of –3.83(4) (C = 1.159 cm^3 K/mol). Such antiferromagnetic interactions are quite unusual in alternated $D^{+\bullet}A^{-\bullet}$ chains built out of decamethylferricinium salts,[20] and should find their origin in a direct overlap between the radical anion species. A close inspection of the X-ray crystal structure of [$Fe(Cp^*)_2$][**1**] reveals indeed a short S•••S contact (3.515 Å) between radical anions running along the *a* direction (Figure 10), to be compared to twice the sulfur van der Waals radius (2 x 1.80 = 3.60 Å). Tight binding calculations[21] of the $\beta_{LUMO\text{-}LUMO}$ interaction energy associated with this overlap interaction between the acceptor's LUMOs amounts to 27.8 meV, a sizeable value consistent with the observed antiferromagnetic response.[22]

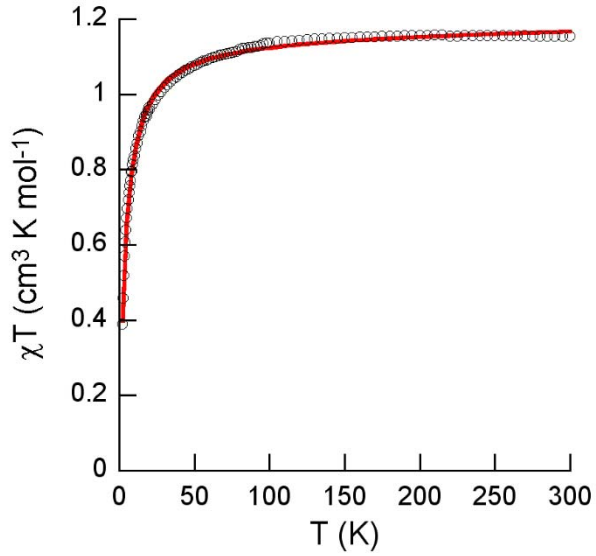

Figure 9. Temperature dependence of the χT product for [Fe(Cp*)$_2$][**1**] at 10000 Oe (with χ defined as molar magnetic susceptibility equal to M/H per [Fe(Cp*)$_2$][**1**] unit). Black circles indicate measured data; red line represents the best fit obtained with the Curie-Weiss model described in the text.

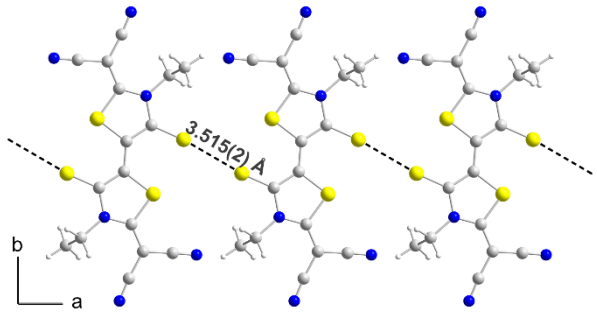

Figure 10. View of the shortest S•••S contacts in the chain of radical anions running along *a* in [Fe(Cp*)$_2$][**1**].

Conclusion

A novel electron acceptor bearing dicyanovinylidene substituents on a bithiazolylidene core has been prepared and characterized. This acceptor exhibits a planar skeleton together with several sulfur atoms which can respectively increase the accepting

ability and enhances intermolecular contacts in the solid state. Association with two different donor molecules, namely tetramethyltetrathiafulvalene (TMTTF) and decamethylferrocene ($Fe(Cp^*)_2$) afforded 1:1 adducts. Analysis of their structural, electrochemical, vibrational and magnetic properties show that [TMTTF][**1**] behaves as a neutral charge-transfer complex while [$Fe(Cp^*)_2$][**1**] is an ionic salt, formulated as [$Fe(Cp^*)_2^+$][$\mathbf{1}^{-\bullet}$]. The presence of the exocyclic sulfur atoms in $\mathbf{1}^{-\bullet}$; together with the concentration of the spin density on these atoms favors the setting of direct antiferromagnetic interactions. Work is now in progress to isolate other salts of reduced **1**, with a specific interest for mixed valence ones as they can potentially lead to highly conduction materials. Besides, the involvement of neutral **1** in field effect transistors will be also considered as good charge mobilities can be anticipated from these favorable overlap interactions.

Experimental section

All commercial chemicals were used without further purification. The solvents were purified and dried by standard methods. All the NMR spectra were obtained in $CDCl_3$ unless indicated otherwise. Chemical shifts are reported in ppm and ^{1}H NMR spectra were referenced to residual $CHCl_3$ (7.26 ppm) or CD_3CN (1.94 ppm) and ^{13}C NMR spectra were referenced to $CHCl_3$ (77.2 ppm) or CD_3CN (118.3 and1.32 ppm). Melting points were measured on a Kofler hot-stage apparatus and are uncorrected. Mass spectra were recorded with Waters Q-Tof 2 instrument by the Centre Régional de Mesures Physiques de l'Ouest, Rennes. Elemental analyses were performed at the Centre Régional de Mesures Physiques de l'Ouest, Rennes. Column chromatography was performed using silica gel Merck 60 (70-260 mesh). DEBTTT was prepared according to literature procedures.[8] Cyclic voltammetry were carried out on a 10^{-3} M solution of **1** in CH_2Cl_2, containing 0.1 M nBu$_4$NPF$_6$ as supporting electrolyte. Voltammograms were recorded at 0.1 Vs^{-1} on a platinum electrode and the

potentials were measured *versus* Saturated Calomel Electrode (SCE). The spectroelectrochemical setup was referenced *versus* SCE in CH_2Cl_2-[NBu_4][PF_6] 0.2 M. A 3600 plus SHIMADZU and FTIR varian 640 IR spectrophotometers were employed to record the UV-vis-NIR and IR spectra.

Synthesis of the protected ligand 4. To a suspension of **2** (500 mg, 1.58 mmol) in chloroform (30 mL) was added trimethylorthoformate (0.69 mL, 6.34 mmol) and borontrifluoride diethylether (1 mL, 7.9 mmol). The reaction mixture was stirred 5 hours at 75°C under nitrogen. The solvent was evaporated *in vacuo*, the oil was washed with diethylether affording **3** as a brown oil which was used in the next step without further purification. Yield: 80%; ^{1}H NMR (CD_3CN, 300 MHz) δ (ppm) = 1.42 (t, 3H, ^3J = 7.3 Hz, CH_2-C$\underline{H}_3$), 2.80 (m, 4H, S-CH_2), 2.92 (s, 3H, S-CH_3), 3.27 (m, 4H, CH_2-CN), 4.49 (q, 2H, ^3J = 7.3 Hz, CH_2); ^{13}C NMR (CD_3CN, 75 MHz) δ (ppm) = 13.0 ($\underline{C}H_3$), 18.6 (S-$\underline{C}H_3$), 18.8 (-$\underline{C}H_2$-CN), 19.1 (-$\underline{C}H_2$-CN), 33.1 (S-$\underline{C}H_2$), 49.7 (CH_2), 119.3 (CN), 138.1 (C=C), 143.4 (C=C), 178.7 ($\underline{C}$-S); HRMS (ESI) calcd for $C^+[C_{12}H_{16}N_3S_4]$: 330.02271 Found: 330.0224. To a suspension of **3** (1.83 g, 4.40 mmol) in dichloromethane, malononitrile (322 mg, 3.99 mmol) and triethylamine (654 µL, 0.76 mmol) were added. The mixture was stirred 5 hours at room temperature under nitrogen atmosphere then washed with 2N HCl (50 mL) and water (3 x 20mL). The concentrated solution was purified by chromatography on silica gel using ethyl acetate and petroleum ether (1:1) as eluent affording **4** as a brown powder. Crystals of sufficient quality were obtained by CH_2Cl_2 slow evaporation. Yield: 32%; Mp: 112°C; ^{1}H NMR (300 MHz) δ 1.43 (t, 3H, ^3J = 7.1 Hz, CH_3), 2.78 (m, 4H, S-CH_2), 3.17 (m, 4H, CH_2-CN), 4.49 (q, 3H, ^3J = 7.1 Hz, CH_2); ^{13}C NMR (75 MHz) δ 15.2 (CH_3), 18.8 ($\underline{C}H_2CN$), 18.9 ($\underline{C}H_2CN$), 31.8 (S-CH_2), 32.4 (S-CH_2), 45.0 (C=$\underline{C}(CN)_2$), 45.2 (N-CH_2), 117.0 (CN), 117.1 (CN), 124.3 (C=C), 138.1 (C=C), 168.5 ($\underline{C}$=C(CN)$_2$); IR $\tilde{\nu}_{(CN)}$= 2172, 2200 and 2253 cm^{-1};

HRMS (ESI) calcd for $[M^{+}Na]^{+}$ $[C_{14}H_{13}N_5NaS_3]$: 370.02308 Found: 370.0234; Anal.calcd for $C_{14}H_{13}N_5S_4$; C: 48.39, H: 3.77, S: 27.68. Found : C: 48.11, H:3.78, S:27.51.

Synthesis of 1. To a 0°C cooled solution of **4** (200 mg, 0.57 mmol) in dry THF (10 mL) was added a solution of LDA freshly prepared from n-BuLi (0.50 mL, 1.26 mmol) and diisopropylamine (0.17 mL, 1.26 mmol) in 10 mL of dry THF. After stirring for 20 min at -20°C, triphosgene (341 mg, 1.15 mmol) was added and the solution was stirred for 12 hours at room temperature. The solvent was evaporated in vacuo and 10 mL of toluene were added on the crude product under nitrogen atmosphere. The mixture was refluxed for 12 hours. The concentrated solution was purified by chromatography on silica gel using CH_2Cl_2 as eluent affording **1** as purple crystals. Crystals of sufficient quality were obtained by slow concentration of a CH_2Cl_2 solution of **1**. Yield: 48%; Mp: >230°C; ^{1}H NMR (300 MHz) δ 1.45 (t, 6H, ^{3}J = 7.1 Hz, CH_3), 4.74 (q, 4H, ^{3}J = 7.1 Hz, CH_2); ^{13}C NMR (75 MHz) δ 14.5 (CH_3), 44.0 (C=C(CN)$_2$), 48.0 (N-CH_2), 111.6 (=C(<u>C</u>N)$_2$), 112.6 (=C(<u>C</u>N)$_2$), 128.1 (C=C), 169.1 (<u>C</u>=C(CN)$_2$), 184.9 (C=S); UV-vis (CH_2Cl_2) λ (nm) Ɛ (L.mol^{-1}cm^{-1}) 366 (23460), 517 (3940); IR $\tilde{\nu}_{(CN)}$ = 2215 cm^{-1}; HRMS (ESI) calcd for $M^{+}.(C_{16}H_{10}N_6S_4)$: 413.98498 Found: 413.98553.

Synthesis of acceptor 1 from DEBTTT. To a 0°C cooled solution of DEBTTT (50 mg, 0.14 mmol) in toluene (15 mL) was added a drop of water and a solution tetracyanoethylene oxide (164 mg, 1.14 mmol) in 5 mL of acetonitrile. The reaction mixture was stirred 3 hours at 0°C and 12 hours at room temperature. The solvent was evaporated *in vacuo* and dichloromethane (80 mL) was added. The solution was washed with water (5×30 mL) and dried over $MgSO_4$. The concentrated solution was purified by chromatography on silica gel using CH_2Cl_2 as eluent affording **1** as purple crystals. Yield: 56%.

Elaboration of [TMTTF][1]. To a hot solution of TMTTF (6 mg, 0.024 mmol) in dichloromethane (10 mL) was added a hot solution of **1** (10 mg, 0.024 mmol) in acetonitrile. The mixture was refluxed for 10 minutes and the solution was allowed to reach room temperature slowly. Slow evaporation of the solution afford deep purple crystals.

Elaboration of [Fe(Cp*)$_2$][1]. To a hot solution of decamethylferrocene (11.74 mg, 0.036 mmol) in toluene (5 mL) was added to a hot solution of **1** (15 mg, 0.036 mmol) in toluene. The mixture was refluxed for 20 minutes. Slow evaporation of the solution afforded dark crystals.

Crystallography. Data were collected on an APEXII, Bruker-AXS diffractometer, for **4**, **1** and [TMTTF][**1**] and on D8 VENTURE Bruker AXS diffractometer for [Fe(Cp*)$_2$][**1**]. Both diffractometers operate with graphite-monochromated Mo-Kα radiation (λ = 0.71073 Å). The structures were solved by direct methods using the *SIR97* program,[23] and then refined with full-matrix least-square methods based on F^2 (*SHELXL-97*)[24] with the aid of the WINGX program.[25] All non-hydrogen atoms were refined with anisotropic atomic displacement parameters. H atoms were finally included in their calculated positions. Crystallographic data on X-ray data collection and structure refinements are given in Table 2 for **1**, **4**, [TMTTF][**1**] at RT, [TMTTF][**1**] at 150K and [Fe(Cp*)$_2$][**1**] (CCDC 1471695-1471699).

Electronic supplementary information (ESI) available: Crystallographic data, CCDC No. 1471695-1471699 and computational details. For ESI and crystallographic data in CIF or other electronic format see DOI:

Table 2 Crystallographic data

Compound	**4**	**1**	[TMTTF][**1**] at RT	[TMTTF][**1**] at 150 K	[Fe(Cp*)$_2$][**1**]
Formula	$C_{14}H_{13}N_5S_3$	$C_{16}H_{10}N_6S_4$	$C_{26}H_{22}N_6S_8$	$C_{26}H_{22}N_6S_8$	$C_{36}H_{40}FeN_6S_4$
FW (g·mol^{-1})	347.47	414.54	674.98	674.98	740.83
Crystal system	monoclinic	triclinic	triclinic	triclinic	monoclinic
Space group	$P\,2_1/c$	$P\bar{1}$	$P\bar{1}$	$P\bar{1}$	$P2_1/n$
a (Å)	9.9664(7)	5.3638(2)	7.2959(11)	7.2379(10)	8.6586(5)
b (Å)	9.6751(6)	7.2562(3)	8.7231(12)	8.6275(12)	20.4937(12)
c (Å)	16.8053(13)	12.7329(5)	12.7388(18)	12.664(2)	10.9221(6)
α (°)	90	77.773(2)	102.719(8)	102.003(8)	90
β (°)	99.922(5)	80.204(1)	101.011(7)	100.361(8)	109.724(2)
γ (°)	90	69.110(1)	91.481(7)	91.428(9)	90
V (Å^3)	1596.23(19)	450.06(3)	774.33(19)	759.30(19)	1824.38(18)
T (K)	150(2)	294(2)	293(2)	150(2)	150(2)
Z	4	1	1	1	2
D_{calc} (g·cm^{-3})	1.446	1.529	1.447	1.476	1.349
μ (mm^{-1})	0.467	0.541	0.605	0.617	0.677
Total refls.	8303	7308	12634	7173	14104
Uniq. refls. (R_{int})	3611(0.0503)	2051 (0.0292)	3442 (0.0368)	3446 (0.0584)	4121(0.0474)
Unique refls.(I>2s(I))	2960	1872	2363	2604	3551
R_1, wR_2	0.0423, 0.099	0.0261, 0.0711	0.0417, 0.1016	0.061, 0.1361	0.0937, 0.2136
R_1, wR_2 (all data)	0.0527, 0.106	0.0292, 0.0747	0.0685, 0.1140	0.0813, 0.1464	0.1067, 0.2203

GoF	1.053	1.053	1.065	1.024	1.279

References

1 (a) N. Martin, *Chem. Commun.,* 2013, **49***,* 7025–7027. (b) P. Batail, P. (Ed.), Special issue on Molecular Conductors, *Chem. Rev*., 2004*,* **104**, 4887–5781.

2 H. Li, T. Earmme, G. Ren, A. Saeki, S. Yoshikawa, N. M. Murari, S. Subramaniyan, M. J. Crane, S. Seki and S. A. Jenekhe, *J. Am. Chem. Soc.,* 2014, **136**, 14589−14597.

3 C. Wang, H. Dong, W. Hu, Y. Liu and D. Zhu, *Chem. Rev.,* 2012, **112**, 2208–2267.

4 H. Usta, A. Facchetti and T. J. Marks, *Acc. Chem. Res.,* 2011, **44**, 501–510.

5 A. R. Murphy and J. M. J. Fréchet, *Chem. Rev.,* 2007, **107**, 1066–1096.

6 (a) R. C. Wheland, *J. Am. Chem. Soc.,* 1976*,* **98**, 3926–3930. (b) G. Saito and J. P. Ferraris, *Bull. Chem. Soc. Jpn*., 1980, 2141–2145**.**

7 K. P. Goetz, D. Vermeulen, M. E. Payne, C. Kloc, L. E. McNeil and O. D. Jurchescu, *J. Mater Chem. C,* 2014, **2**, 3065–3076.

8 Y. Le Gal, N. Bellec, F. Barrière, R. Clérac, M. Fourmigué, V. Dorcet, T. Roisnel and D. Lorcy, *Dalton Trans,* 2013, **42**, 16672–16679.

9 A. Filatre-Furcate, T. Higashino, D. Lorcy and T. Mori, *J. Mater. Chem. C,* 2015, **3**, 3569–3573.

10 Y. Le Gal, D. Ameline, N. Bellec, A. Vacher, T. Roisnel, V. Dorcet, O. Jeannin and D. Lorcy, *Org. Biomol. Chem*., 2015, **13**, 8479–8486.

11 N. Tenn, N. Bellec, O Jeannin, L. Piekara-Sady, P. Auban-Senzier, J. Iniguez, E. Canadell and D. Lorcy, *J. Am. Chem. Soc*., 2009, **131**, 16961–16974.

12 (a) D. Guérin, R. Carlier, D. Lorcy, *J. Org. Chem.,* 2000, **65**, 6069–6072. (b) D. Guérin, R. Carlier, M. Guerro, D. Lorcy, *Tetrahedron,* 2003, **59**, 5273–5278.

13 H. Ohtsuka, T. Miyasaka, K. Arakawa, *Chem. Pharm. Bull.,* 1975, **23**, 3254-3265.

14 W. J. Linn and E. Ciganek, *J. Org. Chem*., 1969, **34**, 2146–2152.

15 R. Gompper, J.-G. Hansel, J. Hock, K. Polborn, E. Dormann and H. Winter, *Mol. Cryst. Liq. Cryst.,* 1995, **273**, 1–16.

16 J. S. Chappell, A. N. Bloch, W. A. Bryden, M. Maxfield, T. O. Poehler and D. O. Cowan, *J. Am. Chem. Soc.,* 1981, **103**, 2442–2243.

17 J. B. Torrance, J. E. Vazquez, J. J. Mayerle and V. Y. Lee, *Phys. Rev. Lett*., 1981, **46**, 253.

18 P. Guionneau, C. J. Kepert, G. Bravic, D. Chasseau, M. R. Truter, M. Kurmoo and P. Day, *Synth. Met.,* 1997, **86**, 1973–1974.

19 A. S. Batsanov, M. R. Bryce, A. Chesney, J. A. K. Howard, D. E. John, A. J. Moore, C. L. Wood, H. Gershtenman, J. Y. Becker, V. Y. Khodorkovsky, A. Ellern, J. Bernstein, I. F. Perepichka, V. Rotello, M. Gray and A. O. Cuello, *J. Mater. Chem.*, 2001, **11**, 2181–2191.

20 (a) J. S. Miller, J. C. Calabrese, H. Rommelmann, S. R. Chittipeddi, J. H. Zhang, W. M. Reiff and A. J. Epstein, *J. Am. Chem. Soc*., 1987, **109**, 769–781; (b) G. T. Yee and J. S. Miller, in *Magnetism: molecules to materials V*, Eds. J. S. Miller and M. Drillon, Wiley, Weinheim, chp. 7, 2005.

21 J. Ren, W. Liang and M.-H. Whangbo, Crystal and Electronic Structure Analysis Using CAESAR; North Carolina State University: 1998.

22 See for example: (a) T. Bsaibess, M. Guerro, Y. Le Gal, D. Sarraf, N. Bellec, M. Fourmigué, F. Barrière, V. Dorcet, T. Guizouarn, T. Roisnel and D. Lorcy, *Inorg. Chem.,* 2013, **52**, 2162−2173 (b) M. Fourmigué, B. Domercq, I. V. Jourdain, P. Molinié, F. Guyon and J. Amaudrut, *Chem. Eur. J.,* 1998, **4**, 1714–1723.

23 A. Altomare, M. C. Burla, M. Camalli, G. Cascarano, C. Giacovazzo, A. Guagliardi, A. G. G. Moliterni, G. Polidori and R. Spagna, *J. Appl. Crystallogr.,* 1999, **32**, 115–119.

24 G. M. Sheldrick, *Acta Cryst.,* 2008, **A64**, 112–122.

25 L. J. Farrugia, *J. Appl. Cryst.,* 2012, **45**, 849–854.

TOC

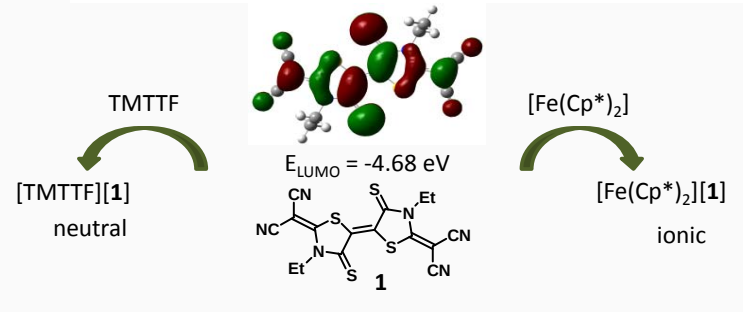

A novel sulfur rich π-electron acceptor affords with electron donors 1:1 adducts: a neutral charge-transfer complex and a paramagnetic ionic salt.